Journal of Physics:
Conference Series

PAPER • **OPEN ACCESS**

Modelling the phantom array from the spatial waveform on the retina

To cite this article: Chan-Su Lee and Arnold J. Wilkins 2025 *J. Phys.: Conf. Ser.* **3128** 012002

Journal of Physics: Conference Series **3128** (2025) 012002 doi:10.1088/1742-6596/3128/1/012002

Modelling the phantom array from the spatial waveform on the retina

Chan-Su Lee[1*], and Arnold J. Wilkins[2]

[1] Department of Electronic Engineering, Yeungnam University, Gyeongsan, Rep. of Korea
[2] Department of Psychology, University of Essex, Colchester, United Kingdom

[*]E-mail: chansu@ynu.ac.kr

Abstract The phantom array effect is one of the artefacts of temporal light modulation (TLM) and has related health issues. This paper presents an analytic model of the visibility of the phantom array effect derived from the spatial contrast sensitivity function (SCSF), typical eye movement speeds, temporal integration according to the light source size, and the Fourier fundamental of the waveform. During a saccadic eye movement, any temporally modulated light source will stimulate spatially disparate regions of the retina according to the modulation frequency, the light source size and eye movement velocity. By integrating over time, we can estimate the shape and contrast of the retinal stimulation and thereby estimate its visibility on the basis of models of contrast sensitivity. The Fourier fundamental of the spatial pattern is used to predict its visibility. Recent experimental datasets of the visibility of the phantom array effect fit well to the model. The model can be extended to explain individual differences, and the spectral dependence of the visibility of the phantom array effect.

1. Introduction

Temporal light modulation (TLM) refers to a fluctuation in the luminous quantity or spectral power distribution of the output of a lighting system over time [1]. The fast response of solid-state light sources makes the effect of TLM more prominent than that of previous lighting sources. In many cases TLMs may give rise to unacceptable annoying effects. These undesirable changes are called temporal light artefacts (TLA) [3]. TLA can be a cause of a decrease of visual performance, an increase in fatigue and health problems like eye-strain [4]. Symptoms of discomfort correlate with the visibility of the threshold frequency of the phantom array effect [5].

The phantom array effect is the appearance of multiple images of objects lit with a temporally varying light source during a rapid eye movement (saccade) [4]. The visibility of the phantom array effect can be influenced by the luminance, modulation frequency, and duty cycle of the modulation [6]. Chromaticity and colour temperature [7], and angular width of the light source [8] are also important.

The visibility threshold frequencies of the phantom array effect show large individual differences [7, 9]. Individual variation of eye movement speed (by a factor of up to two) is one of the factors that can explain large individual variations of the phantom array visibility [10]. Another factor is the four-fold difference in contrast sensitivity within the normally sighted population [11].

There have been several recent parametric studies of the phantom array effect [12, 13]. However, the explanations of the phenomena are limited. We present an analytic model that seeks to explain the variation of the visibility of the phantom array and its dependence on the characteristics of TLM in terms of the spatial waveform on the retina.

2. Modelling the phantom array from the spatial waveform

The spatial waveform generated on the retina during a saccade directed across a source of temporally modulated light can be calculated from the speed of eye movement and the modulation depth and duty cycle of the temporal light modulation (TLM). When the light has a large spatial extent and the frequency of the TLM is high, the light received by the retina from one part of the lamp at one phase in the light's temporal cycle is superimposed on that from a different part and different phase, potentially influencing the modulation depth of the spatial pattern. Both the spatial extent of the lamp and the frequency of TLM are critical.

The spatial frequency of the phantom array can be used to calculate the log contrast sensitivity using one of the published formulae, such as that of Barten [14] or stelaCSF [15]. These formulae apply to free view of a grating, but are due to basic physiological constraints of the visual system. The brevity of the presentation during a saccade and any saccadic suppression may be expected to reduce the visibility, especially when the background is lit. Nevertheless, the greater sensitivity to mid spatial frequencies, as in the Barten equation, is likely to survive such effects, given that it reflects the size of receptive fields of retinal neurons.

Miller et al. [16] report the visibility of a varying light source across which observers make saccades. The duty cycles (DC) and modulation depths (MD) were systematically varied for a range of TLM frequencies, waveforms and modulation depths. Calculation of the spatial waveform, the amplitude of its Fourier fundamental and the log of the associated contrast sensitivity have been undertaken for the data they present and used to predict the visibility of the phantom array.

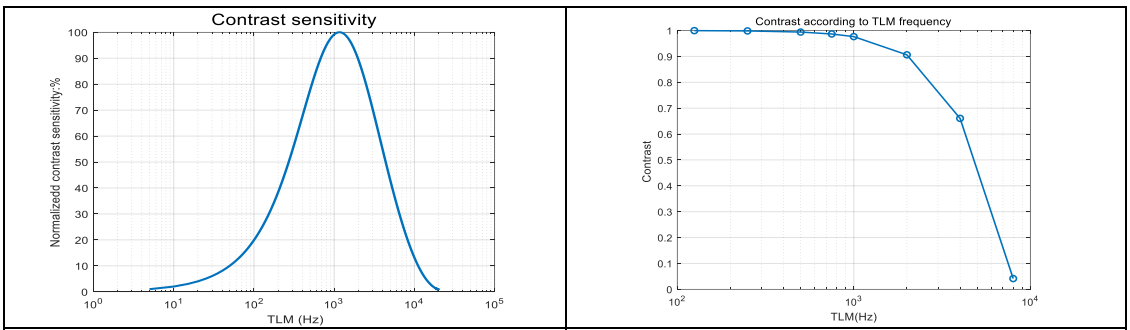

(a) Contrast sensitivity for TLM **(b) Spatially spread TLM contrast**

Figure 1. Spatial contrast sensitivity function with eye movement. (a) Contrast sensitivity as a function of the spatial frequency of the phantom array, as determined by the TLM of the light source and a saccade velocity of 500deg/s. (b) Spatially spread temporal light modulation (TLM) contrast according to modulation frequency.

2.1 Sinusoidal modulation of the light and phantom array visibility from temporal Integration of the spatial waveform

For ease of exposition, we begin with consideration of the condition with sinusoidal modulation of the light. The data from Miller et al. [16] have been modelled assuming a saccade size of 44

degrees, a (constant maximum) velocity of 500deg/s, and a viewing distance of 3000mm, as specified by Miller et al. The luminance of the source was 38,700cd/m^2 and was maintained constant for the various experimental conditions. The width of the LED was 3.2 mm (0.061 degrees). The light energy was spread by the saccade over a 44 degree visual angle, so that the rotational space-averaged luminance of the phantom array used in the Barten [14] equation was taken to be 38700/44*0.061=53.8 cd/m^2. The contrast sensitivity according to the Barten formula was calculated from the spatial period of the waveform and is shown in Figure 1 (a) below as a function of the frequency of TLM for a saccade with a velocity 500deg/s.

When we assume a constant eye movement speed, the retinal trajectory and its duration are fixed. During the trajectory, we can assume that the light source intensity depends only on the light source modulation frequency and modulation depth. In addition, light arriving at the photoreceptors will probably be integrated before the information is passed along the visual pathway.

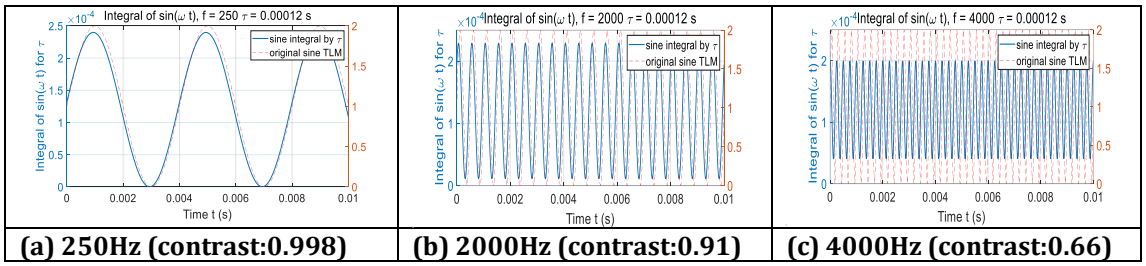

Figure 2. Variation of contrast of the sine wave in different modulation frequency with a constant eye movement speed and a fixed integration time. (a) 250Hz sine wave modulation. (b) 2000Hz sine wave modulation. (c) 4000 Hz sine wave modulation

The sinusoidal signal of the modulation will change its shape due to integration of the signal according to the crossing time of the light source. Figure 2 shows examples of the change of

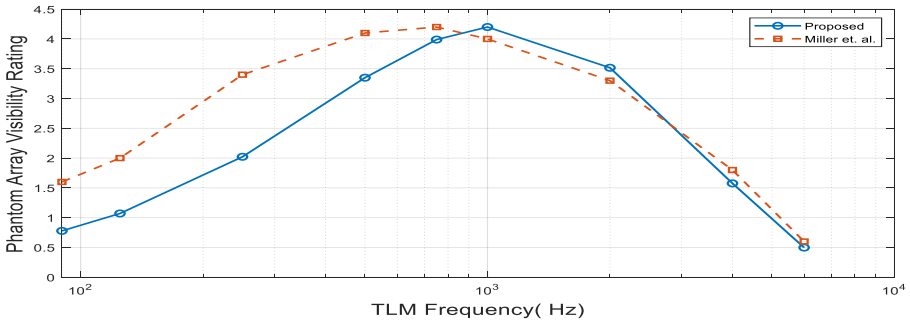

Figure 3. The model and the empirical data for sinusoidal TLM, after Miller et al. [16] Figure 7b.

sinusoidal signal after integration at different modulation frequencies. As a result, the contrast of the signal after integration is decreased with increasing temporal frequency of the TLM because parts of the retinal image of the lamp were superimposed at different phases of the TLM cycle. The contrast of the sinusoid spatial pattern in different TLM frequencies is shown in Figure 1 (b).

The product of the two weighting functions is shown in Figure 3 together with the empirical function from Miller et al. [16], which is shown as a broken line. The two functions have been constrained to have similar origins and similar maxima. The resulting fit is within experimental

error. The poorer fit at low TLM is probably attributable to the velocity profile of the saccade, and the limited time during which the saccade was at its peak velocity. The phantom array at the peak of the saccade velocity (as modelled) will have been flanked by higher spatial frequencies that resulted from the lower saccade velocity either side of the peak. The higher spatial frequencies may have increased the visibility of the phantom array.

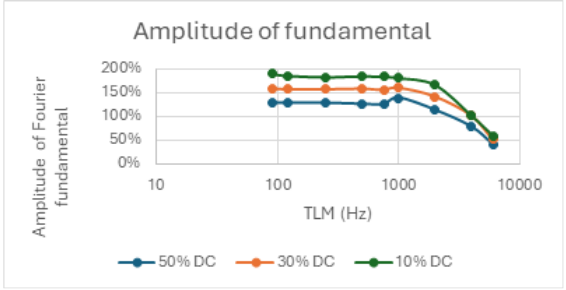

(a) Amplitude of the Fourier fundamental for three duty cycles

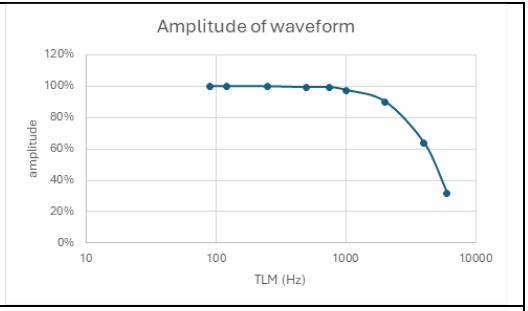

(b) Amplitude of the spatial waveform as a function of TLM frequency

Figure 4. Amplitude of the Fourier fundamental and spatial waveform.

2.2 Rectangular modulation of the light and phantom array visibility from Fourier fundamental of the spatial waveform

Fourier analysis of the spatial waveform can be used to obtain the amplitude of the Fourier fundamental. Higher frequency components may then be ignored, given that they have too high a spatial frequency and too low a contrast to be visible.

The rectangular TLM waveforms used by Miller et al. [16] required an additional calculation.

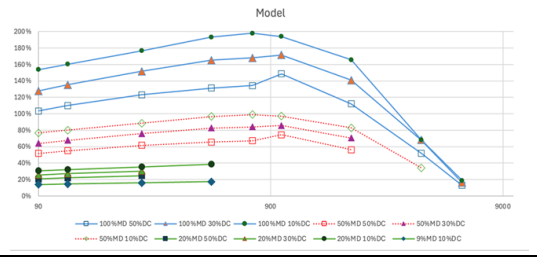

(a) Estimates of the visibility of the phantom array shown as a function of TLM frequency, modulation depth, and duty cycle

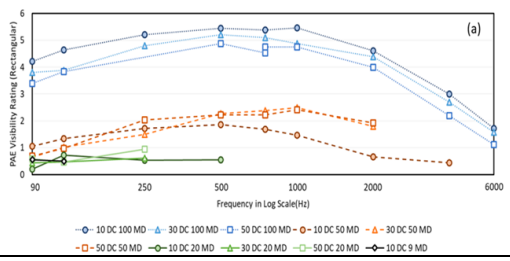

(b) Visibility of the phantom array for rectangular TLM after Miller et al. [16] Figure 7a.

Figure 5. Amplitude of the Fourier fundamental and spatial waveform.

One period of the spatial waveform was derived from the two-dimensional spatio-temporal waveform, and its numerical series used to calculate the amplitude of the Fourier fundamental. This was expressed as a percent of the average amplitude of the numerical series (Figure 4 (a)). The percentage was multiplied by the amplitude of the waveform (Figure 4 (b)) taking account of the modulation depth to derive the amplitude of the Fourier fundamental. This was multiplied by the weighting for contrast sensitivity (Figure 1 (a)).

The product of the modulation depth and the functions in Figures 1 (a), Figure 4 (a) and Figure 4 (b) is shown in Figure 5 (a). This may be compared with the empirical data collected by Miller et al. [16] shown in their Figure 7a, reproduced in Figure 5 (b). The vertical axis of the model is arbitrary but ordinal and most of the empirical data are ordered as predicted by the model. The factors of amplitude and contrast sensitivity, are currently given equal weight.

The empirical data for the 10% duty cycle with 50% modulation depth are not well fit, however. The duration of the stimulus presentation with 10% duty cycle was 0.1ms or less at TLM frequencies of 1kHz and above. In no other condition was the duration so short. Allowance can be made for an insufficiency of light energy. This insufficiency will be in inverse proportion to the light duration, and the downward trajectory of the empirical data can therefore be emulated easily, to resemble that shown in Figure 5 (b).

2.3 Individual differences of the phantom array visibility from individual saccade velocity and contrast sensitivity

There are large individual differences in the perception of the phantom array, and they have a possible significance for health, given that individuals who can best see the array are those who experience eye-strain in everyday life [17]. In normally sighted individuals contrast sensitivity can range over a factor of four [11]. There are also at least two-fold differences in maximum saccade velocity for a given saccade size [10][19]. The large individual differences in perception of the phantom array may perhaps be explained in terms of these two factors: individual difference in saccade velocity and individual difference in contrast sensitivity.

Individual differences in saccade velocity: The peak velocity of a saccade increases with the size of eye movement according to a function known as the main sequence. However, the slope of the main sequence differs from one individual to another [19], so that for a given size of eye

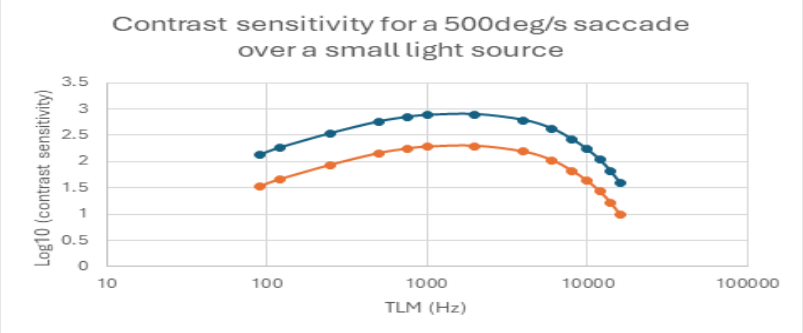

Figure 6. Two contrast sensitivity functions for observers with a saccade velocity of 500 deg/s, the upper curve for an observer with high contrast sensitivity and the lower curve for an observer with low.

movement the velocity can vary by a factor of two [20]. This variation will affect the spatial frequency of the phantom array, and with it, the contrast sensitivity. For high temporal frequencies and consequently high spatial frequencies, the slope of the contrast sensitivity function is steep. An individual with a relatively slow saccade will experience a phantom array with a relatively high spatial frequency which will be more difficult to see, as demonstrated by Kang et al. [10].

Individual differences in contrast sensitivity: Contrast sensitivity is known to vary across the general population by a factor of four [11]. Figure 6 shows two functions for contrast sensitivity

spaced apart by a factor of four. If the size of the lamp is so small that it is unnecessary to consider any overlap of the retinal image (and temporal integration of the images) from one temporal cycle to the next, the upper frequency limit above which the phantom array is visible can be calculated by extrapolation of the known curves. This would indicate an upper limit that is necessarily less than 20kHz. The maximum limit thus far recorded is about 15kHz [19]. When the viewing conditions are such as to require a contrast sensitivity of about 300 (i.e. a log10(contrast sensitivity) ~ 2.5) in order to see the phantom array, the array will be visible to the observer with high contrast sensitivity between about 200Hz and about 800Hz, a large range, but will not be visible to the observer with the low contrast sensitivity at any frequency.

3. Conclusion and Future works

In this paper, we presented new models from the spatial waveform on the retina using temporal integration and the Fourier fundamental. The validity of the proposed model supported the similarity of the conventionally measured visibility model of the phantom array effect from Miller et. al.[16].

There are other factors that affect the phantom array visibility such as target size [8] and spectral distribution of the light source [7][8][21]. We need to extend the model to explain the effect of such factors to obtain a general model of phantom array visibility.

We plan to extend the model to account for other factors such as the spectral distribution and the large individual variations of the visibility of the phantom array effect. In addition, the proposed model can be extended to other TLM analytic visibility such as the stroboscopic effect.

4. Acknowledgements

The authors are grateful for discussions with Dr J G Robson.

References

[1] Commission International de l'Eclairage. Technical Note TN 012:2021 2021 Vienna Guidance on the Measurement of Temporal Light Modulation of Light Sources and Lighting Systems
[2] CIE 249:2022 2022 Visual aspects of time-modulated lighting systems
[3] CIE TN006:2016 2016 Visual aspects of time-modulated lighting systems.
[4] IEEE Std 1789:2015 2015 Recommended Practices of Modulating Current in High Brightness LEDs for Mitigating Health Risks to Viewers
[5] Boyce PR and Wilkins A Visual discomfort indoors 2018 *Lighting Research & Technology* **50**(1), 98–114.
[6] Vogels I, Hernando I 2012 Effect of eye movements on perception of temporally modulated light *Proceedings of Experiencing Light*
[7] Kang HR, Kim JG, Park SW, Lee C-S and Park H 2022 Visibility of the Phantom Array Effect at Different LED Colour Temperatures Under High-Frequency Temporal Light Modulation *Lighting Research and Technology* **55**(1), 36–46
[8] Park SW, Lee C-S, Kang HR, Park H and Wilkins A 2019 Visibility of the phantom array effect according to luminance, chromaticity and geometry *Lighting Research and Technology* **52**(3), 377–388
[9] Wang LL, Tu Y, Cheng SL, Yu XL, Perz M and Sekulovski D 2019 The visibility of the phantom array effect under office lighting condition *Proceedings of CIE* 17-21
[10] Kang H, Lee CS, Kim JG and Pak H 2023 Saccadic eye movement speed is related to variations in phantom array effect visibility *Sci. Rep.* **13** 11576
[11] Baker DH. 2013 What is the primary cause of individual differences in contrast sensitivity? *PLoS ONE* **8**(7) e69536
[12] Lee C-S and Kang H 2023 An analytic approach to the visibility model of the phantom array effect, *Proc. Of CIE*

[13] Brűckner S and Khanh TQ 2007 A field experiment on the perception of automotive rear lights using pulsed LEDs with different frequencies *Proceedings of International Symposium on Automotive Lighting* 25–26
[14] Barten PG 2003 Formula for the contrast sensitivity of the human eye *Proc. SPIE* **5294** 231–238
[15] Mantiuk RK, Ashraf M and Chapiro A 2022 stelaCSF – A unified model of contrast sensitivity as the function of spatio-temporal frequency, eceentricity, luminance and area *ACM Trasn. Graph.* **41**(4) 1–16
[16] Miller N, Rodriguez-Feo Bermudez E, Irvin L and Tan J 2023 Phantom array and stroboscopic effect visibility under combinations of TLM parameters *Lighting Research & Technology* **56**(7) 707–733
[17] Brown E, Foulsham T, Lee C-S and Wilkins A 2020 Visibility of temporal light artefact from flicker at 11kHz *Lighting Research and Technology*, **52** 371-376
[18] Gibaldi A and Sabatini SP 2021 The saccade main sequence revised: A fast and repeatable tool for oculomotor analysis *Behav Res Methods* **53**(1) 167-187
[19] Kang H, Lee C-S, Lee J and Lee K-M 2023 Phantom array effect can be observed above 15 kHz in high speed eye movement group for high luminance warm white LED *Lighting Research & Technology* **56**(7) 669-675
[20] Kong X, Vogels R, Martinsons C, Tengelin M and Heynderickx I 2023 Dependence of temporal frequency and chromaticity on the visibility of the phatom array effect *Proc. of CIE* 347-356